ENERGY AND POWER OF NONLINEAR WAVES IN A SEVEN-STORY REINFORCED CONCRETE BUILDING

V. Gicev* and Mihailo D. Trifunac**

*Rudarsko-Geoloski Fakultet
Goce Delcev 89, 2000 Stip, Republic of Macedonia
**Department of Civil Engineering
University of Southern California, Los Angeles, CA 90089, U.S.A.

ABSTRACT

We note the limitations of the classical Response Spectrum Method (RSM) for the design of earthquake-resistant structures in the near field of strong earthquakes. The main limitation is that the RSM is based on the largest peak of the relative response and does not consider the duration of strong motion. To illustrate an alternative approach the recorded response of a seven-story reinforced concrete hotel (VN7SH) in Van Nuys, California, damaged during January 1994, Northridge earthquake is described in terms of one-dimensional layered shear beam model, undergoing nonlinear wave excitation. We use this model to show the time and space variations of wave energy and of power in the building response, and to set a physical basis for a new design method based on the power of strong motion pulses propagating through a building.

KEYWORDS: Earthquake Response Spectra, Power of Incident Waves, Power Design Method

INTRODUCTION

"The problem of designing structures to withstand destructive earthquakes is not in a very satisfactory condition. On the one hand engineers do not know what characteristics of the ground motion are responsible for destruction, and on the other hand seismologists have no measurements of seismic motion which are sufficiently adequate to serve for design, even if the destructive characteristics were known. Consequently, engineers have been forced to proceed on an empirical basis. From past experience … it has been found that buildings, which are designed to withstand a constant horizontal acceleration of 0.1 gravity are, on the whole, fairly resistant to seismic damage. It is fortunate that such a simple formula works at all …" (Benioff, 1934).

Modern earthquake engineering began with the formulation of the concept of response spectrum by Biot, who presented the general theory (Biot, 1932, 1933, 1934), analyzed the recorded accelerograms, and formulated the principles of response spectrum superposition (Biot, 1941, 1942). Today, three quarters of a century later, his ideas still govern the principles of earthquake-resistant design (Trifunac, 2003, 2005). Biot's method works well for the design of structures expected to vibrate without damage. However, pragmatic considerations and optimization of cost result in the design of structures, which may experience damage from a rare and very strong earthquake shaking. Thus, during the past 40 years, many modifications and "corrections" have been introduced into the Biot's response spectrum method to reconcile its "linear" nature with its desired "nonlinear" use in design (Veletsos and Newmark, 1960).

At present much of the earthquake-resistant design continues to be based on the linear concepts of relative response spectrum, and on mode superposition. However, as used in practice, the modal approach has a low-pass filtering effect on the end result (e.g., the computed peak relative displacement at each floor) because in design the higher modes are usually neglected. Therefore, in typical earthquake engineering applications the modal approach is not able to represent the sudden transient response. This is particularly so for the excitation by high-frequency pulses in the near-field, with large peak velocities, which are associated with high stress drop at the near asperities, and with duration that is short relative to the travel time required for an incident wave to reach the top of the building. Although, in principle, the representation of the linear response as a combination of the modal responses is mathematically complete, short "impulsive" representation would require considering infinitely many modes, which is impractical. The wave propagation methods are therefore more "natural" for representing the "early" transient response, and should be used to find solutions where the modal approach is limited.

Well-designed structures are expected to have uniformly distributed "ductile behavior" during the largest credible shaking, and "large energy reserve" to at least delay failure if it cannot be avoided. As the structure enters large nonlinear response, it absorbs the excess of the input energy by ductile deformation of its components. Thus, it is logical to formulate earthquake-resistant design procedures in terms of the energy driving this process. Benioff (1934) proposed the seismic destructiveness to be measured in terms of the response energy, which also can be related to the energy of strong motion (Arias, 1970; Trifunac and Brady, 1975). Thus an alternative to the spectral method in earthquake-resistant design is to analyze the flow of energy during the strong motion. The principal stages of this flow include the earthquake source, the propagation path, and finally the remaining energy, which leads to the response of a structure (Trifunac et al., 2001c).

The seismic energy associated with the elastic waves that radiate from the source (Gutenberg and Richter, 1956a, 1956b) can be used to compare "sizes" of different earthquakes. This energy, E_s, is attenuated along the epicentral distance r through the mechanisms of inelastic attenuation (Trifunac, 1994), scattering, and geometric spreading. The wave energy arriving towards the site is next attenuated by the nonlinear response of shallow sediments and soil in the "free-field" (Joyner, 1975; Joyner and Chen, 1975; Trifunac and Todorovska, 1996, 1998a, 1999) before it begins to excite the foundation. The incident wave energy is further reduced by the nonlinear response of soil during the soil-structure interaction (Gicev, 2005; Trifunac et al., 1999a, 1999b, 2001a, 2001b), and by the radiation damping (Luco et al., 1986; Todorovska and Trifunac, 1991, 1992; Hayir et al., 2001).

Engineering analyses of seismic energy flow and distribution among different aspects of the structural response have been carried out since the mid-1950's. A review of the subject and examples describing the "limit-state" design can be found in the book by Akiyama (Akiyama, 1985), and in the collection of papers edited by Fajfar and Krawinkler (Fajfar and Krawinkler, 1992), for example. In most engineering studies, the analysis begins by integrating the differential equation of dynamic equilibrium of an equivalent single-degree-of-freedom system with respect to displacement, which results in

$$E_I = E_K + E_\varsigma + E_E + E_H \tag{1}$$

where E_I is the input energy, E_K is the kinetic energy, E_ς is the damping energy, E_E is the elastic strain energy, and E_H is the hysteretic energy (e.g., Uang and Bertero, 1988). A typical limitation of this approach is that the computed energy is essentially converted to the peak relative velocity (Akiyama, 1985), thus using energy merely to compute the equivalent relative velocity spectra, and then the classical response spectrum superposition method is used. Further the effects of soil-structure interaction are ignored, and therefore significant mechanisms of energy loss (via nonlinear response of the soil and radiation damping) are neglected, leading to erroneous inferences about the energy available to drive the structural response. Other simplifications and important omissions in Equation (1) are that the dynamic instability and the effects of gravity on the nonlinear response are usually ignored (Husid, 1967; Lee, 1979; Todorovska and Trifunac, 1991, 1993).

Figure 1 illustrates the cumulative wave energies recorded at a building site during two hypothetical earthquakes (see the demands E1 and E2), and presents the conceptual framework for development of the power design method. E1 results in a larger total shaking energy at the site, and has long duration of shaking leading to relatively small average power, P1. E2 leads to smaller total shaking energy at the site, but has short duration and thus larger power, P2. The power capacity of a structure cannot be described by one unique cumulative curve, as this depends on the time history of shaking. For the purposes of this example, the line labeled "capacity envelope of the structure" can be thought of as an envelope of all possible cumulative energy paths for the response of this structure. Figure 1 implies that E1 will not damage this structure, but E2 will. Hence, "for a given structure, it is not the total energy of an earthquake event (and the equivalent energy compatible relative velocity spectrum), but the rate with which this energy arrives and shakes the structure, that is essential for the design of the required power capacity of the structure to withstand this shaking, and to control the level of damage" (Trifunac et al., 2001c).

In this paper elementary aspects of response, based on the energy and power of the wave motion, are illustrated. It will be shown how this power can be compared with the temporal and spatial capacity of the structure to absorb the incident wave energy.
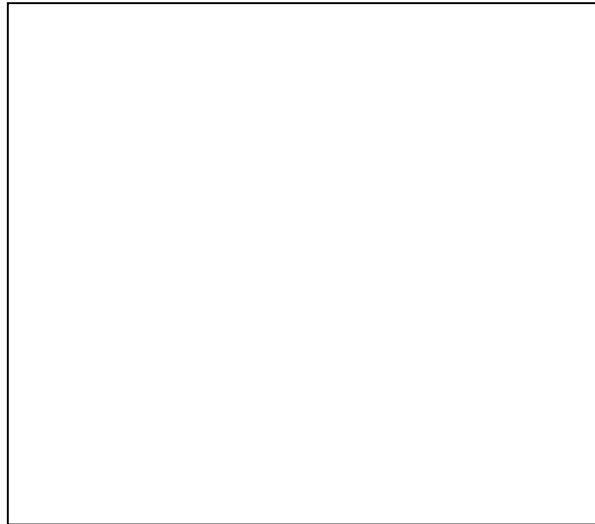
Fig. 1   Comparison of the strong motion demands E1 and E2 with an envelope of structural capacity

CASE STUDY—VAN NUYS HOTEL (VN7SH)

The example building used in this study is a seven-story hotel (VN7SH) located in Van Nuys, California. It was damaged by the 1994 Northridge, California earthquake (Ivanović et al., 1999a, 1999b; Trifunac and Hao, 2001; Trifunac et al., 1999a, 1999b). The building, designed in 1965 and constructed in 1966 (John A. Blume & Associates, 1973; Mulhern and Maley, 1973), is 18.9×45.7 m in plan, has seven stories, and is 20 m high. The typical framing consists of four rows of columns spaced at 6.1 m centers in the transverse direction and nine columns of columns at 5.7 m centers in the longitudinal direction. Spandrel beams surround the perimeter of the structure. Lateral forces in the longitudinal (EW) direction are resisted by the interior column-slab frames (B and C) and exterior column spandrel beam frames (A and D). The added stiffness in the exterior frames associated with the spandrel beams creates exterior frames that are roughly twice as stiff as the interior frames. The floor system consists of reinforced concrete flat slab, which is 25.4 cm thick at the second floor, 21.6 cm thick at the third to seventh floors, and 20.3 cm thick at the roof (Browning et al., 2000; De la Llera et al., 2001; Islam, 1996; Li and Jirsa, 1998; Trifunac and Ivanović, 2003). The building is situated on undifferentiated Holocene alluvium, uncemented and unconsolidated, with a thickness of < 30 m and an age of < 10,000 years (Trifunac and Todorovska, 1998b). The average shear-wave velocity in the top 30 m of soil is 300 m/s, and the soil-boring log shows that the underlying soil consists primarily of fine sandy silts and silty fine sands. The foundation system consists of 96.5-cm deep pile caps, supported by groups of two to four poured-in-place 61-cm-diameter reinforced concrete friction piles. These are centered under the main building columns. All of the pile caps are connected by a grid of beams. Each pile is approximately 12.2 m long and has a design capacity of over 444.82×10^3 N vertical load and up to 88.96×10^3 N lateral load. The structure is constructed of normal-weight reinforced concrete ((John A. Blume & Associates, 1973).

1. Earthquake Damage

The $M_L = 6.4$ Northridge earthquake of January 17, 1994 severely damaged the building. The structural damage was extensive in the exterior north (D) (see Figure 2(a)) and south (A) (see Figure 2(b)) frames that were designed to take most of the lateral load in the longitudinal (EW) direction. Severe shear cracks occurred at the middle columns of Frame A, near the contact with the spandrel beam of the 5th floor (see Figure 2(b)). Those cracks significantly decreased the axial, moment, and shear capacity of the columns. The shear cracks that appeared in the north (D) frame (see Figure 2(a)) caused minor to moderate changes in the capacities of these structural elements. No major damage to the interior longitudinal (B and C) frames was observed, and there was no visible damage to the slabs or around the foundation. The nonstructural damage was significant. Photographs and detailed descriptions of the damage from the earthquake can be found in Trifunac et al. (1999b) and Trifunac and Hao (2001). An analysis of the relationship between the observed damage and the changes in the equivalent vertical shear-

wave velocity in the building can be found in Ivanović et al. (1999b) and Todorovska and Trifunac (2006). A discussion of the extent to which this damage has contributed to the changes in the apparent period of the soil-structure system can be found in Trifunac et al. (2001a, 2001b).

2. Strong-Motion Records

The earthquake response of VN7SH was recorded by a 13-channel CR-1 central recording system, and by one tri-component SMA-1 accelerograph (see Figure 3) with an independent recording system but with common trigger time with the CR-1 recorder (Trifunac et al., 1999b). The five transducers, which recorded EW response of the building during the earthquake, were located at the ground (first), second, third, and sixth floors, and on the roof (see Figures 2(a), 2(b) and 3).

Fig. 2(a) Observed damage of Frame D

3. Previous Work

Two full-scale ambient vibration tests of VN7SH were performed (Ivanović et al., 1999a, 2000) following the earthquake. During the second ambient vibration survey, measurements of wave motion through the building foundation showed that the foundation is "flexible" and deforms with the passage of micro-tremor waves. This in turn indicated that for the studies of soil-structure interaction the rigid foundation assumption may not be appropriate (Trifunac et al., 1999a). The apparent period of the soil-structure system and its dependence upon the response amplitudes in VN7SH were described by Trifunac et al. (2001a, 2001b), and an application of off-line and on-line identification techniques to the building response data in VN7SH was presented by Loh and Lin (1996). A continuum mechanics representation of VN7SH in terms of isotropic and anisotropic two-dimensional models and their response to incident wave motion was considered by Todorovska et al. (2001a, 2001b). The feasibility of identifying the observed damage through wave propagation studies using recorded earthquake responses was explored in Ivanović et al. (1999b), Trifunac et al. (2003), and Todorovska and Trifunac (2006).

The engineering studies of VN7SH have focused mainly on its longitudinal (EW) response. Without exception, these studies have neglected the effects of soil-structure interaction and have implicitly assumed that all nonlinearities in the observed response are associated with the building structure.

Fig. 2(b) Observed damage of Frame A

Fig. 3 Location of CR-1 channels (1-13), and of SMA-1 accelerographs (14-16)

Islam (1996) considered two two-dimensional models for EW response of the building. Assuming the building to be fixed at the ground floor level, he used the triangular distributed horizontal load to perform a push-over analysis. Figure 4 shows his results for *V/W*, the resulting base shear (*V*), normalized by the appropriate fraction of building weight (*W*), versus the roof displacement, assuming that the south perimeter frame (A) resists one third of the lateral load. Islam (1996) concluded, "many of the structural elements may have exceeded their elastic limit state at approximately 4 s into the earthquake. However, the most severe damage, e.g., breakdown of the entire load path in the south perimeter frame columns immediately below the 5th floor level, may have actually occurred at approximately 9 s, which coincides with the time of the peak ground acceleration in the longitudinal direction". He also notes, "a push-over analysis performed on the longitudinal frame with a triangular load pattern was unable to predict the damage observed in the building".
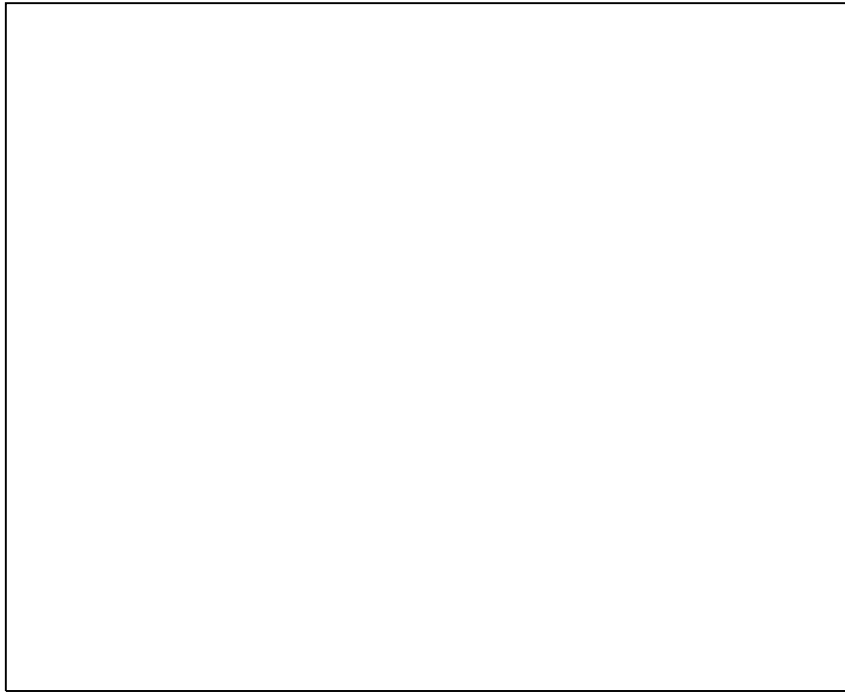
Fig. 4   Base shear (*V*) coefficient, normalized by total building weight *W*, versus EW roof displacement of VN7SH (open circles indicate the first occurrence of nonlinear strain at the floors 1 through 7 as obtained in this study)

Li and Jirsa (1998) performed a "nonlinear time history" analysis of VN7SH in the longitudinal (EW) direction "only because most of the damage occurred in this direction". Acceleration time histories recorded at ground level were used as the input ground motion, and columns were assumed to be fixed at the base. Soil-structure interaction was not included in the models. Effective stiffness and residual lateral capacity were chosen so that the period of calculated response-time history would match the recorded time history, and $0.35EI_g$ was chosen as an effective stiffness for all beams and columns. Their analysis was two-dimensional, and therefore no torsional effects of excitation and of response could be included. Li and Jirsa stated, "push-over analysis successfully predicted that the structure almost lost its lateral load-resisting capacity, and the shear failures of columns occurred prior to reaching the maximum roof displacement the building experienced during the earthquake".

Browning et al. (2000) compared three independent analyses, including their own results, with regard to the response of VN7SH to the Northridge earthquake: Approach A (by Lynn and Moehle); Approach B (by Browning and Sozen); and Approach C (by Li and Jirsa). Because Approach C has already been summarized, we mention briefly only the results of the analyses based on the approaches A and B. Approach A idealizes the building as a two-dimensional frame and considers only the longitudinal (interior and exterior) framing lines. A simple bi-linear relation without stiffness or strength degradation is used to describe load-deformation properties of the frames. The foundation is assumed to be rigid, i.e., no soil-structure interaction is considered, and the authors used triangular load distribution with monotonically increasing amplitude in their push-over analysis (Figure 4). Dynamic "nonlinear response histories" were computed for the motion measured at the base of the building. Approach B used geometry of the model similar to that in Approach A, but the in-fill walls were assumed not to contribute to resistance to the lateral forces. A "Takeda nonlinear model" with unloading stiffness reduction equal to 0.4 was adopted, and nonlinear static and dynamic response analyses were conducted. The results of the push-over analysis are shown in Figure 4.

De la Llera et al. (2001) noted, "planar analyses of the building reported previously are obviously not capable of predicting ... torsional motion". They developed an idealization of the building consisting of a "single column-like element" (SEM) connecting two consecutive floors, and used this model to interpret the three-dimensional response of the VN7SH building to the earthquake. As in all previous investigations of the response of this building, De la Llera et al. (2001) ignored the soil-structure interaction effects in their analyses of translational and torsional responses.

NONLINEAR WAVES

Wave propagation models of buildings have been used for many years (Kanai, 1965), but are only recently beginning to be verified against observations (Ivanović et al., 1999b; Todorovska et al., 2001a, 2001b, 2001c; Trifunac and Todorovska, 2001; Trifunac et al., 2001c). Continuous, 2-D wave propagation models (i.e., homogeneous, horizontally layered and vertically layered shear plates) can be employed to study the effects of traveling waves on the response of long buildings (Todorovska et al., 1988; Todorovska and Trifunac, 1989, 1990a, 1990b; Todorovska and Lee, 1989). Discrete-time 1-D wave propagation models were proposed to study the response of tall buildings (Gilstrap et al., 1998), and 2-D finite difference methods were used to study linear and nonlinear soil-structure interaction (Gicev, 2005).

In the following the elementary principles of wave propagation through a layered shear beam model will be used to demonstrate the relationships between the power of incident strong ground motion and of the building response.

1. The Building Model

We consider a one-dimensional finite difference model, and use the velocity of shear waves and the density of the slabs and inter-story columns based on the analysis of the impulse response for EW recorded motions in Holiday Inn hotel (Todorovska and Trifunac, 2006). These parameters together with the inter-story heights, as adopted in this study, are summarized in Table 1. As can be seen from this table, the stiffness and the density of the floors is much larger than the stiffness of the columns. Therefore it can be expected that the floors will move essentially as rigid bodies. The yielding and the nonlinear characteristics of the material have been estimated previously from the east-west response of this model by assuming that the input ground motion can be approximated by strong motion recorded at the first (ground) floor (i.e., at the channel 16). We did this by comparing the computed motions with the recorded motions at higher floors in the building (i.e., at the channel 12 at the second floor, channel 11 at the third floor, channel 10 at the sixth floor, and at the channel 9 at the roof) (Gicev and Trifunac, 2006b). The location of the instruments in the building, which recorded the EW response, is shown in Figure 3. By varying the yielding strain and the strengthening factor γ, assuming that they are same for the whole building, and by minimizing the error between the recorded and the calculated responses, we obtained the best estimates for the yielding strain $\varepsilon_y = 0.0025$ and $\gamma = 0.44$. These two parameters together with those in Table 1 then complete the description of our finite difference bilinear model parameters (Gicev and Trifunac, 2006b).

Table 1: One-Dimensional Building Model

	Interstory Height $h_{\text{interstory}}$ (m)	Slab Thickness h_{slab} (m)	$\beta_{\text{interstory}}$ (m/s)	β_{slab} (m/s)	$\rho_{\text{interstory}}$ (kg/m³)	ρ_{slab} (kg/m³)
Roof Slab		0.203		2000		2384
Seventh Story	2.44		73.15		82.90	
Seventh Floor Slab		0.215		2000		2384
Sixth Story	2.44		76.20		82.90	
Sixth Floor Slab		0.216		2000		2384
Fifth Story	2.44		77.72		82.90	
Fifth Floor Slab		0.216		2000		2384
Fourth Story	2.44		79.25		82.90	
Fourth Floor Slab		0.216		2000		2384
Third Story	2.44		91.44		82.90	
Third Floor Slab		0.216		2000		2384
Second Story	2.44		129.50		82.90	
Second Floor Slab		0.254		2000		2384
First Story	3.86		140.20		76.92	

In this paper, we adopt the same model parameters but consider the one-dimensional interaction between the soil and the building by taking two more spatial points in the soil (Gicev and Trifunac, 2006a). We further assume that the soil is linear having shear wave velocity β_s = 300 m/s and density ρ_s = 2000 kg/m^3. We assume that the horizontal wave motion in the ground propagates upward and that it is the one recorded at the channel 16 (see Figure 5). Of course, this is not the actual incident wave motion during the Northridge main event, because the record in the channel 16 resulted from the incident and reflected wave-field at the base of the building. Also this record contains the soil-structure interaction effects. Nevertheless, using this record as an approximation for the arriving waves in the ground we can approximately study the overall features of the response of the building during the main event of the Northridge earthquake from the energy point of view. In all other respects our modeling of the building by the one-dimensional finite difference model is identical to the one described in Gicev and Trifunac (2006a), and its description is, therefore, not repeated here.
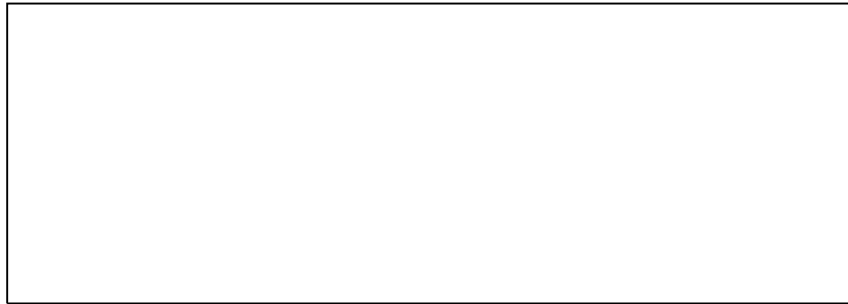

Fig. 5 Incident ground motion

2. Results

2.1 Energy Distribution in the Model

Because the model we study represents a conservative system, the kinetic and elastic parts of the potential energy, the energy that radiated out from the building into the soil, and the energy spent for development of the permanent strains in the building must add up to the incident wave energy. In   Figure 6 the energy that radiated out of the building into the soil, E_{out}, and the energy spent on the work leading to the permanent strains, E_{hys}, are shown versus time. The energy is computed in kilojoules (1 kJ = 1 kN-m), while the time is shown in seconds.
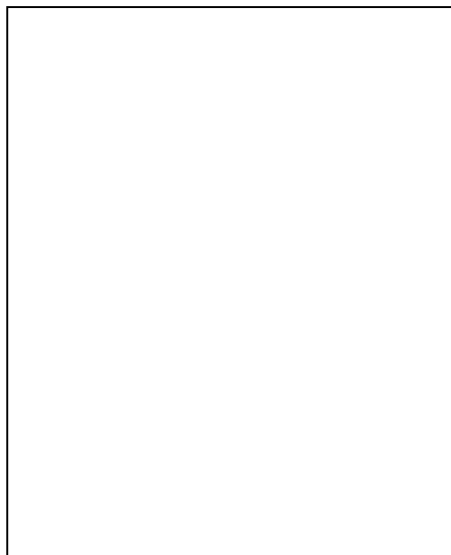

Fig. 6   Energy distribution in VN7SH during the Northridge earthquake (the spent energy consisting of the energy going out of the building and the spent hysteretic energy balance the input energy)

The input energy E_{in} is computed from the input displacement record (as in Figure 5). First, by differentiation of the displacement record with respect to time, the input particle velocity is obtained. The input energy, assuming that the cross section of the model is $A = 1 \text{ m}^2$, is computed assuming vertically propagating one-dimensional plane waves,

$$E_{in} = \rho_s \beta_s \int_0^T v^2 dt \cong \rho_s \beta_s \sum_{k=1}^M v_k^2 \Delta t \qquad (2)$$

where ρ_s and β_s are the density and the shear wave velocity of the soil; $v = \partial u_0 / \partial t$ is the input particle velocity; T is the time at the end of the record; k is the order number of a time-step; $M = T / \Delta t$ is the discrete time at the end of the record; and $v_k = (u_{0,k} - u_{0,k-1}) / \Delta t$ for $k > 1$, and $v_1 = u_{0,1} / \Delta t$ for $k = 1$, are the discrete particle velocities.

The output energy E_{out} is computed from the velocity of the wave going downward, v_{out} (Gicev and Trifunac, 2006a). The cumulative output energy is then computed as

$$E_{out} = \rho_s \beta_s \int_0^T v^2 dt \cong \rho_s \beta_s \sum_{k=1}^M \left(v_{out}^k \right)^2 \Delta t \qquad (3)$$

The hysteretic energy E_{hys} is the energy spent on the development of permanent strains in the building. The hysteretic loop (see Figure 7) represents the relation $\sigma(\varepsilon)$ at a point during one cycle of the response, $T_{0,i} < t < T_{0,i+1}$, where $T_{0,1} = 4 \sum_{j=1}^{14} (h_j / \beta_j) \approx 0.8$ s can be used to approximate the apparent period of the building. Depending upon the input ground motion and the time during the strong motion, the loop can be narrower or wider. By adding the areas of those loops, and assuming no strength reduction due to repetitive loads, we can compute the energy spent for the development of permanent strains at a point. Next, we generalize this for a layer (i.e., a continuous equivalent representation of the columns and walls at a given floor) and for the whole building. The hysteretic energy for a certain layer is obtained as the sum of the loops at the points belonging to that layer, while the hysteretic energy for the whole building is obtained as the sum of the energies in all layers. The hysteretic energy in the building in discrete time space is computed as

$$E_{hys} = \sum_{i=3}^N \Delta x_i \sum_{k=1}^M \sigma_{av}^k \Delta \varepsilon^k \qquad (4)$$

where the indices i and k stand for the spatial and temporal discrete points in the model; N is the point representing the top of the building; M is the point representing the end of the record; $\sigma_{av}^k = (\sigma^k + \sigma^{k-1}) / 2$ is the average stress at a point i in the time-step k; and $\Delta \varepsilon^k$ is the strain-increment at the point i in the kth time-step. The points in the slabs do not contribute to the hysteretic energy because those are assumed to remain linear and to only transmit the wave energy to the layers above and below. As can be seen from Figure 6, after about $t = 30$ s, there is a negligible growth of all energies, and therefore in the following analysis we consider only the first 30 s of strong motion.

Subtracting from the input energy (see Equation (2)), the output (radiated) energy (see Equation (3)), we obtain the instantaneous energy in the building, E_b (see Figure 8). The difference,

$$E_{el}^b = E_b - E_{hys} \qquad (5)$$

then represents the instantaneous elastic (linear) energy in the building. All these energies are computed in kJ. In the bottom of Figure 8, the derivatives (power) of these three energies are shown versus time. The power is shown in kilowatts (1 kW = 1 kJ/s = 1 kN-m/s). Until the end of the record, one part of the elastic energy is radiated, contributing to the output energy E_{out}, and one part is later spent for the development of permanent strains contributing to the hysteretic energy E_{hys}. A part of the energy in the building is reversible. During the loading a fraction of the elastic energy is transformed into the hysteretic energy, and during the unloading a part of the hysteretic energy is converted back into the elastic energy.
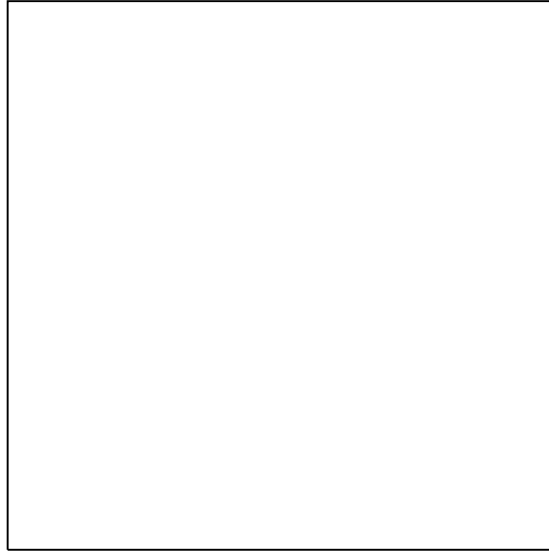
Fig. 7 Hysteresis loop representing $\sigma(\varepsilon)$ during the time $T_{0,i} < t < T_{0,i+1}$
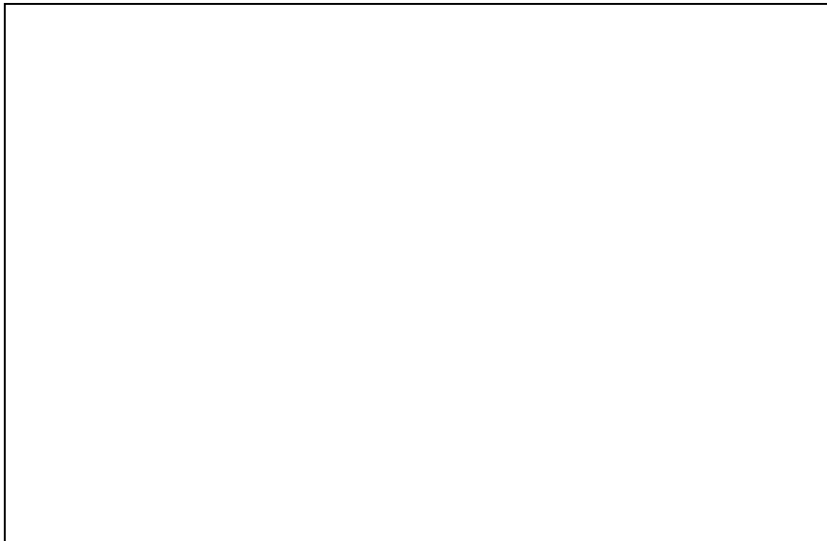

Fig. 8 Energy E_b (top) and power P_b (bottom) in the VN7SH building during the Northridge earthquake, where $E_{\text{el}}^b = E_b - E_{\text{hys}}$

2.2 Energy and Power Capacities and Demands in the Building

To study how the VN7SH building performed during the Northridge earthquake, we consider the energy and the power capacities of different floors. To determine the energy capacity for one period, E_{T_0}, we consider the hysteretic loop at a point, during which the point reaches the strain, ε_u (see Figure 9). The area of the loop A_i is the energy capacity of the floor i for that ε_u and for one period,

$$A_i = E_{T_0}^i = 4 A_{\text{OABB'}} = 4 \cdot \overline{\text{OB'}} \cdot \overline{\text{AA'}} \cdot h_i \tag{6}$$

where h_i is the height of the ith floor. From Figure 9 there follows

$$\overline{\text{AA'}} = \left(\mu_{0i} \varepsilon_{yb} - \mu_{1i} \varepsilon_{yb} \right) \cos \alpha_{1i} \quad \text{and} \quad \overline{\text{OB'}} = \frac{\varepsilon_u - \varepsilon_{yb}}{\cos \alpha_{1i}} \tag{7a}$$

where $\mu_{1i} = \gamma \mu_{oi}$, and the ductility is

$$d = \frac{\varepsilon_u}{\varepsilon_{yb}} \tag{7b}$$

Combining Equation (7a) with Equation (6) the energy capacity of the floor i for one cycle becomes

$$E_{T_0}^i = 4\mu_{0i}\varepsilon_{yb}^2(1-\gamma)(d-1) \tag{8}$$

While the energy capacity for one cycle gives information about the capacity of the floor for an oscillatory loading, the energy capacity of the floor i during one-quarter period, E_q^i, gives information about the resistance of the floor during a single monotonic loading. From Figure 9 this energy corresponds to the area of $\overline{\text{OABB}''}$, consisting of two triangles and one rectangle,

$$A_{\text{OABB}''} = A_{\text{OAA}''} + A_{\text{A}''\text{AB}''\text{B}''} + A_{\text{ABB}''} \tag{9}$$

From Figure 9,

$$E_q^i = \left[\frac{\mu_{0i}\varepsilon_{yb}^2}{2} + \mu_{0i}\varepsilon_{yb}\left(\varepsilon_u - \varepsilon_{yb}\right) + \frac{\gamma\mu_{0i}\left(\varepsilon_u - \varepsilon_{yb}\right)^2}{2} \right] h_i \tag{10}$$

and on using $\varepsilon_u = d\varepsilon_{yb}$ we obtain

$$E_q^i = \frac{\mu_{0i}\varepsilon_{yb}^2}{2}\left[1 + 2(d-1) + \gamma(d-1)^2 \right] \tag{11}$$

The energy capacity of the whole building is the sum of the energy capacities of the inter-story layers,

$$E_{T_0}^b = \sum_i E_{T_0}^i; \ i = 1,3,5,...,13 \tag{12}$$

$$E_q^b = \sum_i E_q^i; \ i = 1,3,5,...,13 \tag{13}$$

The power is the derivative of the energy with respect to time. We compute the power capacity per full cycle by dividing Equation (8) by the period of the building, T_0, and the power capacity for one-quarter cycle by dividing Equation (11) by $T_0/4$,

$$P_{T_0}^i = 4\mu_{0i}\varepsilon_{yb}^2(1-\gamma)(d-1)/T_0 \tag{14}$$

$$P_q^i = 2\mu_{0i}\varepsilon_{yb}^2\left[1 + 2(d-1) + \gamma(d-1)^2 \right]/T_0 \tag{15}$$

From Equations (14) and (15) it can be seen that the power capacity for one full period is linearly dependent upon the ductility d, while the power capacity for one-quarter period (i.e., during loading only) depends upon the square of the ductility. The dependence of the power capacity of the building on its ductility is illustrated in Figure 10. The cumulative growths of normalized hysteretic energies in time for each floor and for the whole building are shown in Figure 11.
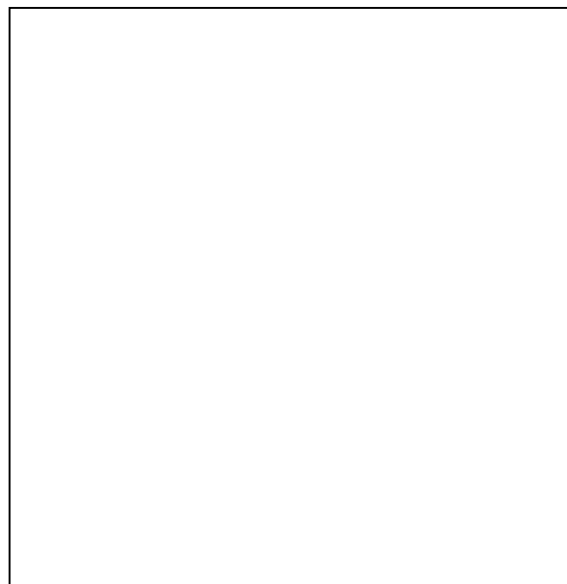

Fig. 9 Hysteresis loop at the strain ε_u during one period of response
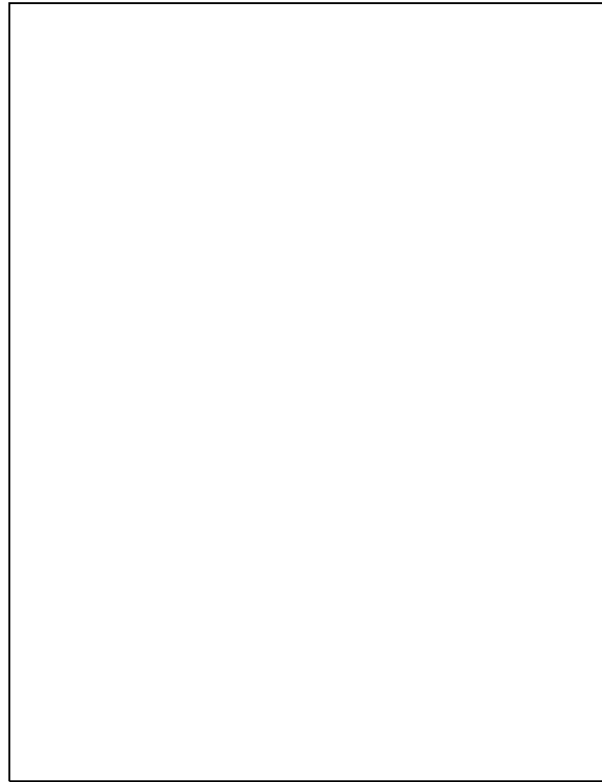
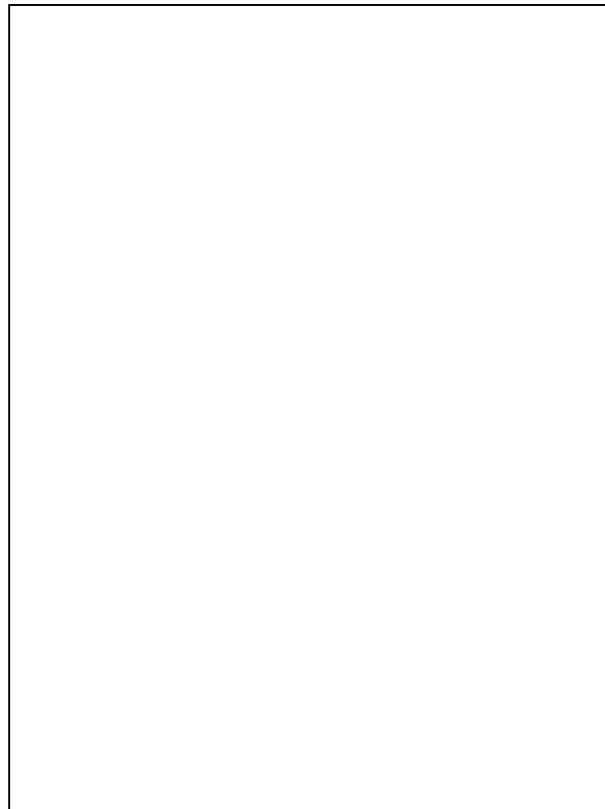Fig. 10 Power capacities for VN7SH for one and one-quarter periods

Fig. 11 Normalized cumulative hysteretic energies E_{hys}/E_c versus time in seven layers (floors) and in the whole building

Trifunac et al. (2001c) estimated input velocity in the building for the equivalent SDOF system that will cause failure, by equalizing the input power in the building and its apparent (i.e., based on actual observation of earthquake effects) power capacity. Following this approach, to understand failure, we

may compare the maximum power in the floor/building with the power capacity of the floor/building. In Figure 11 the cumulative hysteretic energies during the Northridge earthquake for all inter-story layers are presented during the first thirty seconds of strong motion, after normalization (division) by the energy capacities for the ductility $d = 10$. The cumulative energy capacities, computed from Equation (8), can be approximated by straight lines as

$$E_{cT_0}^i(t) = E_{T_0}^i \frac{t}{T_0} \tag{16}$$

where t is the time when the energy capacity of the ith column for one full period is computed, and T_0 is the period of the building. The approximation by Equation (16) is a straight line, with the slope $E_{T_0}^i / T_0$, which represents the power capacity for a full cycle of response. Figure 11 then shows the evolution of the process at each floor. For small oscillations in the beginning of the strong motion, the power demand is small and the maximum capacity of the floors is not mobilized. With the arrival of large strong motion pulses (at about 4 and 9 s after the trigger time), large nonlinear deformations occur with $E_{hys} / E_{c(d=10)}$ exceeding 1.0.

The ductility demands for this model of VN7SH have been calculated by Gicev and Trifunac (2006b), for different floors, and are summarized in Table 2. The maximum strains occurred during the time interval 8.5 s ≤ t ≤ 9.5 s.

Table 2: Peak Ductilities $|d|_{max}$ computed by Gicev and Trifunac (2006b)

Interstory Layer, i	$|d|_{max}$
1	4.10
2	3.67
3	8.64
4	9.39
5	9.39
6	6.73
7	3.71

From Figure 11 it can be seen that the cumulative hysteretic energies $E_{hys}(t)$ (see Equation (4)), normalized with respect to the energy capacities $E_c(t)$ (see Equation (16)) for ductility $d = 10$, for example, are in good agreement with the previously computed maximum ductilities for the same building and for the same excitation, as shown in Table 2 (Gicev and Trifunac, 2006b).

The hysteretic energy demand takes into account only the strains, but does not consider the time rates of change in those strains. In contrast, the power takes into account the energy rates in time, which we compute as derivatives of the energy, after normalization by the rates representing capacity (per unit time T_0 for P_{T0}) for one hysteretic cycle, or by the rates representing capacity (per unit time $T_0/4$ for P_q) for one monotonic loading interval.

Figure 11 shows that at the fourth and the fifth floors, the hysteretic energy, starting from $t = 4$ s, becomes larger than the energy capacity E_c for $d \sim 5$, while it exceeds the energy capacity for $d = 10$ only in a short interval around $t = 9$ s. The energy demand for the whole building is slightly higher than the energy capacity for $d \sim 3.5$ in the interval 8.5 s $< t < 20$ s.

Figures 12(a) and 12(b) show a more detailed view of the physical nature of the demands and of the capacities for two time windows, from 3 to 6 s and from 8 to 11 s, in terms of relative power. In these figures relative power is plotted in terms of the ratio of P_{hys}, which is the time rate of change of E_{hys} (see Equation (4)), normalized (divided) by $P_{c,quart}$ (see Equation (15)) and calculated for $d = 10$. It is seen that this power ratio approaches 2 at the 4th and 7th floors, while at the 5th and 6th floors it is near 3 around 4 s. At the 3rd, 4th, 5th and 6th floors, this ratio exceeds 1 around 5.2 s. The same ratio exceeds 5, for example, at the 3rd, 4th, 5th, and 6th floors between 8.5 and 8.8 s, and again at the 5th floor around 9.2 s.

The largest peak of the ratio $P_{\mathrm{hys}} / P_{c,\mathrm{quart}}$ (for $d = 10$) occurred on the 4th floor, with amplitude larger than 8, at about 8.6 s. These results are in excellent agreement with the location of the observed post-earthquake damage on the same floor (see Figures 2(a) and 2(b)), and with the analyses of the peak strains and peak drifts in the response of the one-dimensional model of VN7SH to the Northridge earthquake (Gicev and Trifunac, 2006b).

Further perusal of the largest peaks of the power ratio, $P_{\mathrm{hys}} / P_{c,\mathrm{quart}}$ (for $d = 10$) (see Figures 12(a) and 12(b)), will show that those occur in sequence, at progressively higher floors, and at the times following the entrance of the strong pulses from the ground motion into the building. The local peak ratios occur in Figure 12(a) around 4 s (at the floors 3, 4, 5, and 6), around 5.2 s (at the floors 1, 2, 3, 4, 5 and 6), and in Figure 12(b) around 8.4 s (at the floors 1, 2, 3, 4, 5, and 6), 9.3 s (at the floors 4, 5 and 6), and 10.3 s (at the floors 3, 4, 5, 6 and 7). As they propagated up into the building, these power pulses caused damage along their path, whenever and wherever the power ratio exceeded the value of about 2. From the time delays between these consecutive pulses in Figures 12(a) and 12(b), we can estimate the average wave speeds associated with the propagation of their energies. Around 4 and 5 s (in Figure 12(a)) this speed is about 40 m/s. Around 8.5 s and 10.2 s (in Figure 12(b)) this speed is lower, about 30 m/s. Comparing these speeds with the initial (linear) velocities in our model (see Table 1), which are in the range from 73 m/s (at the seventh story) to 91 m/s (at the third story) and 140 m/s (at the first story), it can be concluded that those lower speeds resulted from nonlinear deformations in the model. Their values and their times of occurrence are consistent with the results of other direct (see Table 2 and Figure 11 in Todorovska and Trifunac (2008a)) and indirect analyses of the nonlinear waves in VN7SH (Gicev and Trifunac, 2006b; Todorovska and Trifunac, 2006), and show trends similar to what has been seen in other buildings damaged by the strong-motion waves (Todorovska and Trifunac, 2007a, 2007b, 2008b).

SUMMARY AND CONCLUSIONS

Biot's response spectrum method uses characteristic functions (mode shapes) to represent vibrations of a multi-degree-of-freedom system via a set of equivalent single-degree-of-freedom oscillators. Superposition of modal responses is then used to compute actual system response and the peak of that response is employed in earthquake-resistant design to construct envelopes of maximum relative responses (thus defining maximum drift) or of maximum inter-story forces. Mathematically this approach is complete, and the representation in terms of modal responses converges to the exact linear response. However, the simplifications imposed by the design practice result in the use of only the lowest modes of response. The consequence is that the amplitudes of dynamic response to sudden, high-frequency excitation by a near-field pulse are seriously underestimated. For large strong-motion amplitudes the above approach breaks down as the representation in terms of a superposition of modal responses ceases to be valid for the nonlinear response.

When the motion of the structure can be approximated via one-dimensional shear beam idealization (i.e., the contribution of rotational waves can be neglected), we have shown how by comparing the power of a pulse entering the structure (i.e., the demand) with the ability of structure to absorb this power (i.e., the capacity), one can lead to simple and direct estimation of the required structural capacity.

Power (i.e., energy and its duration) of the strong near-field pulses will determine whether the wave entering the structure will continue to propagate through the structure as a linear wave, or will begin to create nonlinear zones (first near the top, and/or near the base of the structure (Gicev, 2005)). For high-frequency pulses the nonlinear zone with permanent strains can be created before the wave motion reaches the top of the structure, i.e., before the interference of waves has even started to occur leading to the formation of mode shapes. Overall duration of the strong motion (Trifunac and Novikova, 1994) will determine the number of times the structure may be able to complete full cycles of response and the associated number of "minor" excursions into the nonlinear response range, when the response is weakly nonlinear (Gupta and Trifunac, 1996), while the presence of powerful pulses of strong motion will determine the extent to which the one-directional quarter-period responses may lead to excessive ductility demand, leading to dynamic instability and failure, precipitated by the gravity loads (Husid, 1967). All these possibilities can be examined and quantified deterministically by the computation of the associated power capacities and power demands for different scenarios for given recorded or synthesized strong motion accelerograms, or probabilistically by extending the methods developed for the uniform hazard analysis (Todorovska et al., 1995).
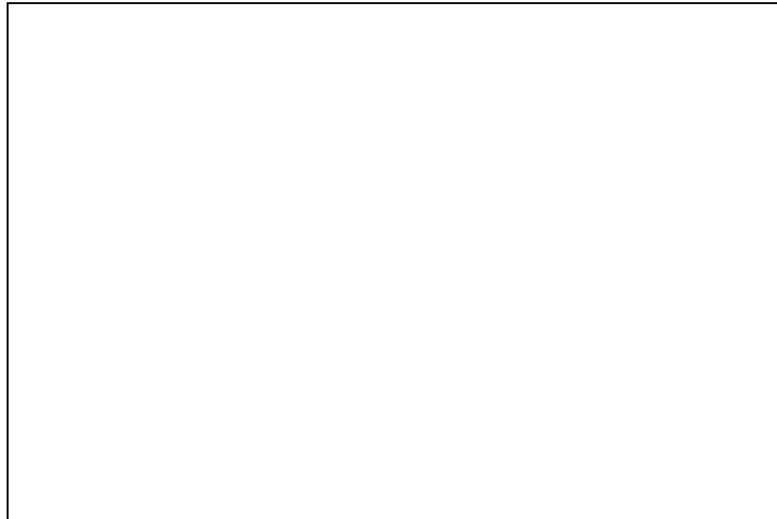
Fig. 12(a)　Normalized power demands in the model of VN7SH building during excitation by the Northridge earthquake, shown separately at the seven floors and in the whole building, for $3 < t < 6$ s

Fig. 12(b)　Normalized power demands in the model of VN7SH building during excitation by the Northridge earthquake, shown separately at the seven floors and in the whole building, for $8 < t < 11$ s

REFERENCES

1. Akiyama, H. (1985). "Earthquake-Resistant Limit-State Design for Buildings", University of Tokyo Press, Tokyo, Japan.

2. Arias, A. (1970). "A Measure of Earthquake Intensity" in "Seismic Design in Nuclear Power Plants (edited by R.J. Hansen)", The MIT Press, Cambridge, U.S.A.

3. Benioff, H. (1934). "The Physical Evaluation of Seismic Destructiveness", Bulletin of the Seismological Society of America, Vol. 24, No. 4, pp. 398-403.

4. Biot, M.A. (1932). "Transient Oscillations in Elastic Systems", Ph.D. Thesis No. 259, Aeronautics Department, California Institute of Technology, Pasadena, U.S.A.

5. Biot, M.A. (1933). "Theory of Elastic Systems Vibrating under Transient Impulse with an Application to Earthquake-Proof Buildings", Proceedings of the National Academy of Sciences of the United States of America, Vol. 19, No. 2, pp. 262–268.

6. Biot, M.A. (1934). "Theory of Vibration of Buildings during Earthquake", Zeitschrift für Angewandte Matematik und Mechanik, Vol. 14, No. 4, pp. 213–223.

7. Biot, M.A. (1941). "A Mechanical Analyzer for the Prediction of Earthquake Stresses", Bulletin of the Seismological Society of America, Vol. 31, No. 2, pp. 151–171.

8. Biot, M.A. (1942). "Analytical and Experimental Methods in Engineering Seismology", ASCE Transactions, Vol. 108, pp. 365–408.

9. Browning, J.A., Li, R.Y., Lynn, A. and Moehle, J.P. (2000). "Performance Assessment for a Reinforced Concrete Frame Building", Earthquake Spectra, Vol. 16, No. 3, pp. 541–555.

10. De la Llera, J.C., Chopra, A.K. and Almazan, J.L. (2001). "Three-Dimensional Inelastic Response of an RC Building during the Northridge Earthquake", Journal of Structural Engineering, ASCE, Vol. 127, No. 5, pp. 482–489.

11. Fajfar, P. and Krawinkler, H. (editors) (1992). "Nonlinear Seismic Analysis and Design of Reinforced Concrete Buildings", Elsevier Applied Science, London, U.K.

12. Gicev, V. (2005). "Investigation of Soil-Flexible Foundation-Structure Interaction for Incident Plane SH Waves", Ph.D. Dissertation, Department of Civil Engineering, University of Southern California, Los Angeles, U.S.A.

13. Gicev, V. and Trifunac, M.D. (2006a). "Rotations in the Transient Response of Nonlinear Shear Beam", Report CE 06-02, University of Southern California, Los Angeles, U.S.A.

14. Gicev, V. and Trifunac, M.D. (2006b). "Non-linear Earthquake Waves in Seven-Storey Reinforced Concrete Hotel", Report CE 06-03, University of Southern California, Los Angeles, U.S.A.

15. Gilstrap, J.M., Dolan, C.W. and Safak, E. (1998). "New Approach to Analyzing Soil-Building Systems", Soil Dynamics and Earthquake Engineering, Vol. 17, No. 7, pp. 509–517.

16. Gupta, I.D. and Trifunac, M.D. (1996). "Investigation of Nonstationarity in Stochastic Seismic Response of Structures", Report CE 96-01, University of Southern California, Los Angeles, U.S.A.

17. Gutenberg, B. and Richter, C.F. (1956a). "Earthquake Magnitude, Intensity, Energy, and Acceleration", Bulletin of the Seismological Society of America, Vol. 46, No. 2, pp. 105–145.

18. Gutenberg, B. and Richter, C.F. (1956b). "Magnitude and Energy of Earthquakes", Annali di Geofisica, Vol. 9, No. 1, pp. 1–15.

19. Hayir, A., Todorovska, M.I. and Trifunac, M.D. (2001). "Antiplane Response of a Dike with Flexible Soil-Structure Interface to Incident SH Waves", Soil Dynamics and Earthquake Engineering, Vol. 21, No. 7, pp. 603–613.

20. Husid, R. (1967). "Gravity Effects on the Earthquake Response of Yielding Structures", Ph.D. Dissertation, California Institute of Technology, Pasadena, U.S.A.

21. Islam, M.S. (1996). "Analysis of the Response of an Instrumented 7-Story Nonductile Concrete Frame Building Damaged during the Northridge Earthquake", Proceedings of the 1996 Annual Meeting of the Los Angeles Tall Buildings Structural Design Council, Los Angeles, U.S.A., Paper No. 96-9.

22. Ivanović, S.S., Trifunac, M.D., Novikova, E.I., Gladkov, A.A. and Todorovska, M.I. (1999a). "Instrumented 7-Storey Reinforced Concrete Building in Van Nuys, California: Ambient Vibration Surveys Following the Damage from the 1994 Northridge Earthquake", Report CE 99-03, University of Southern California, Los Angeles, U.S.A.

23. Ivanović, S.S., Trifunac, M.D. and Todorovska, M.I. (1999b). "On Identification of Damage in Structures via Wave Travel Time", Proceedings of the NATO Advanced Research Workshop on Strong Motion Instrumentation for Civil Engineering Structures, Istanbul, Turkey, pp. 447–468.

24. Ivanović, S.S., Trifunac, M.D., Novikova, E.I., Gladkov, A.A. and Todorovska, M.I. (2000). "Ambient Vibration Tests of a Seven-Story Reinforced Concrete Building in Van Nuys, California, Damaged by the 1994 Northridge Earthquake", Soil Dynamics and Earthquake Engineering, Vol. 19, No. 6, pp. 391–411.

25. John A. Blume & Associates (1973). "Holiday Inn" in "San Fernando, California, Earthquake of February 9, 1971 (edited by L.M. Murphy), Vol. I, Part A", National Oceanic and Atmospheric Administration, U.S. Department of Commerce, Washington, DC, U.S.A.

26. Joyner, W.B. (1975). "A Method for Calculating Nonlinear Seismic Response in Two Dimensions", Bulletin of the Seismological Society of America, Vol. 65, No. 5, pp. 1337–1357.

27. Joyner, W.B. and Chen, A.T.F. (1975). "Calculation of Nonlinear Ground Response in Earthquakes", Bulletin of the Seismological Society of America, Vol. 65, No. 5, pp. 1315–1336.

28. Kanai, K. (1965). "Some Problems of Seismic Vibration of Structures", Proceedings of the Third World Conference on Earthquake Engineering, Wellington, New Zealand, Vol. II, pp. 260–275.

29. Lee, V.W. (1979). "Investigation of Three-Dimensional Soil-Structure Interaction", Report CE 79-11, University of Southern California, Los Angeles, U.S.A.

30. Li, R.Y. and Jirsa, J.D. (1998). "Nonlinear Analyses of an Instrumented Structure Damaged in the 1994 Northridge Earthquake", Earthquake Spectra, Vol. 14, No. 2, pp. 265–283.

31. Loh, S.-H. and Lin, H.-M. (1996). "Application of Off-line and On-line Identification Techniques to Building Seismic Response Data", Earthquake Engineering & Structural Dynamics, Vol. 25, No. 3, pp. 269–290.

32. Luco, J.E., Wong, H.L. and Trifunac, M.D. (1986). "Soil-Structure Interaction Effects on Forced Vibration Tests", Report CE 86-05, University of Southern California, Los Angeles, U.S.A.

33. Mulhern, M.R. and Maley, R.P. (1973). "Building Period Measurements before, during and after the San Fernando Earthquake" in "San Fernando, California, Earthquake of February 9, 1971 (edited by L.M. Murphy), Vol. I, Part B", National Oceanic and Atmospheric Administration, U.S. Department of Commerce, Washington, DC, U.S.A.

34. Todorovska, M.I. and Lee, V.W. (1989). "Seismic Waves in Buildings with Shear Walls or Central Core", Journal of Engineering Mechanics, ASCE, Vol. 115, No. 12, pp. 2669–2686.

35. Todorovska, M.I. and Trifunac, M.D. (1989). "Antiplane Earthquake Waves in Long Structures", Journal of Engineering Mechanics, ASCE, Vol. 115, No. 12, pp. 2687–2708.

36. Todorovska, M.I. and Trifunac, M.D. (1990a). "A Note on the Propagation of Earthquake Waves in Buildings with Soft First Floor", Journal of Engineering Mechanics, ASCE, Vol. 116, No. 4, pp. 892–900.

37. Todorovska, M.I. and Trifunac, M.D. (1990b). "Note on Excitation of Long Structures by Ground Waves", Journal of Engineering Mechanics, ASCE, Vol. 116, No. 4, pp. 952–964.

38. Todorovska, M.I. and Trifunac, M.D. (1991). "Radiation Damping during Two-Dimensional In-plane Building-Soil Interaction", Report CE 91-01, University of Southern California, Los Angeles, U.S.A.

39. Todorovska, M.I. and Trifunac, M.D. (1992). "The System Damping, the System Frequency and the System Response Peak Amplitudes during In-plane Building-Soil Interaction", Earthquake Engineering & Structural Dynamics, Vol. 21, No. 2, pp. 127–144.

40. Todorovska, M.I. and Trifunac, M.D. (1993). "The Effects of Wave Passage on the Response of Base-Isolated Buildings on Rigid Embedded Foundations", Report CE 93-10, University of Southern California, Los Angeles, U.S.A.

41. Todorovska, M.I. and Trifunac, M.D. (2006). "Impulse Response Analysis of the Van Nuys 7-Story Hotel during 11 Earthquakes (1971–1994): One-Dimensional Wave Propagation and Inferences on Global and Local Reduction of Stiffness due to Earthquake Damage", Report CE 06-01, University of Southern California, Los Angeles, U.S.A.

42. Todorovska, M.I. and Trifunac, M.D. (2007a). "Earthquake Damage Detection in the Imperial County Services Building I: The Data and Time-Frequency Analysis", Soil Dynamics and Earthquake Engineering, Vol. 27, No. 6, pp. 564–576.

43. Todorovska, M.I. and Trifunac, M.D. (2007b). "Earthquake Damage Detection in the Imperial County Services Building II: Analysis of Novelties via Wavelets", Soil Dynamics and Earthquake Engineering (under review).

44. Todorovska, M.I. and Trifunac, M.D. (2008a). "Impulse Response Analysis of the Van Nuys 7-Storey Hotel during 11 Earthquakes and Earthquake Damage Detection", Structural Control and Health Monitoring, Vol. 15, No. 1 (in press).

45. Todorovska, M.I. and Trifunac, M.D. (2008b). "Earthquake Damage Detection in the Imperial County Services Building III: Analysis of Wave Travel Times via Impulse Response Functions", Soil Dynamics and Earthquake Engineering (in press).

46. Todorovska, M.I., Lee, V.W. and Trifunac, M.D. (1988). "Investigation of Earthquake Response of Long Buildings", Report CE 88-02, University of Southern California, Los Angeles, U.S.A.

47. Todorovska, M.I., Gupta, I.D., Gupta, V.K., Lee, V.W. and Trifunac, M.D. (1995). "Selected Topics in Probabilistic Seismic Hazard Analysis", Report CE 95-08, University of Southern California, Los Angeles, U.S.A.

48. Todorovska, M.I., Ivanović, S.S. and Trifunac, M.D. (2001a). "Wave Propagation in a Seven-Story Reinforced Concrete Building: Part I. Theoretical Models", Soil Dynamics and Earthquake Engineering, Vol. 21, No. 3, pp. 211–223.

49. Todorovska, M.I., Ivanović, S.S. and Trifunac, M.D. (2001b). "Wave Propagation in a Seven-Story Reinforced Concrete Building: Part II. Observed Wavenumbers", Soil Dynamics and Earthquake Engineering, Vol. 21, No. 3, pp. 225–236.

50. Todorovska, M.I., Hayir, A. and Trifunac, M.D. (2001c). "Antiplane Response of a Dike on Flexible Embedded Foundation to Incident SH-Waves", Soil Dynamics and Earthquake Engineering, Vol. 21, No. 7, pp. 593–601.

51. Trifunac, M.D. (1994). "Q and High-Frequency Strong Motion Spectra", Soil Dynamics and Earthquake Engineering, Vol. 13, No. 3, pp. 149–161.

52. Trifunac, M.D. (2003). "23rd ISET Annual Lecture: 70-th Anniversary of Biot Spectrum", ISET Journal of Earthquake Technology, Vol. 40, No. 1, pp. 19–50.

53. Trifunac, M.D. (2005). "Scientific Citations of M.A. Biot" in "Poro-Mechanics III: Biot Centennial (1905–2005) (edited by Y.N. Abousleiman, A.H.-D. Cheng and F.-J. Ulm)", A.A. Balkema, London, U.K.

54. Trifunac, M.D. and Brady, A.G. (1975). "A Study on the Duration of Strong Earthquake Ground Motion", Bulletin of the Seismological Society of America, Vol. 65, No. 3, pp. 581–626.

55. Trifunac, M.D. and Hao, T.Y. (2001). "7-Storey Reinforced Concrete Building in Van Nuys, California: Photographs of the Damage from the 1994 Northridge Earthquake", Report CE 01-05, University of Southern California, Los Angeles, U.S.A.

56. Trifunac, M.D. and Ivanović, S.S. (2003). "Analysis of Drifts in a Seven-Story Reinforced Concrete Structure", Report CE 03-01, University of Southern California, Los Angeles, U.S.A.

57. Trifunac, M.D. and Novikova, E.I. (1994). "State of the Art Review on Strong Motion Duration", Proceedings of the Tenth European Conference on Earthquake Engineering, Vienna, Austria, Vol. 1, pp. 131–140.

58. Trifunac, M.D. and Todorovska, M.I. (1996). "Nonlinear Soil Response—1994 Northridge, California, Earthquake", Journal of Geotechnical Engineering, ASCE, Vol. 122, No. 9, pp. 725–735.

59. Trifunac, M.D. and Todorovska, M.I. (1998a). "Nonlinear Soil Response as a Natural Passive Isolation Mechanism—The 1994 Northridge, California, Earthquake", Soil Dynamics and Earthquake Engineering, Vol. 17, No. 1, pp. 41–51.

60. Trifunac, M.D. and Todorovska, M.I. (1998b). "Damage Distribution during the 1994 Northridge, California, Earthquake Relative to Generalized Categories of Surficial Geology", Soil Dynamics and Earthquake Engineering, Vol. 17, No. 4, pp. 239–253.

61. Trifunac, M.D. and Todorovska, M.I. (1999). "Reduction of Structural Damage by Nonlinear Soil Response", Journal of Structural Engineering, ASCE, Vol. 125, No. 1, pp. 89–97.

62. Trifunac, M.D. and Todorovska, M.I. (2001). "Recording and Interpreting Earthquake Response of Full-Scale Structures", Proceedings of the NATO Advanced Research Workshop on Strong Motion Instrumentation for Civil Engineering Structures, Istanbul, Turkey, pp. 131–155.

63. Trifunac, M.D., Ivanović, S.S., Todorovska, M.I., Novikova, E.I. and Gladkov, A.A. (1999a). "Experimental Evidence for Flexibility of a Building Foundation Supported by Concrete Friction Piles", Soil Dynamics and Earthquake Engineering, Vol. 18, No. 3, pp. 169–187.

64. Trifunac, M.D., Ivanović, S.S. and Todorovska, M.I. (1999b). "Seven Story Reinforced Concrete Building in Van Nuys, California: Strong Motion Data Recorded between 7 February 1971 and 9 December 1994, and Description of Damage Following Northridge, 17 January 1994 Earthquake", Report CE 99-02, University of Southern California, Los Angeles, U.S.A.

65. Trifunac, M.D., Ivanović, S.S. and Todorovska, M.I. (2001a). "Apparent Periods of a Building. I: Fourier Analysis", Journal of Structural Engineering, ASCE, Vol. 127, No. 5, pp. 517–526.

66. Trifunac, M.D., Ivanović, S.S. and Todorovska, M.I. (2001b). "Apparent Periods of a Building. II: Time-Frequency Analysis", Journal of Structural Engineering, ASCE, Vol. 127, No. 5, pp. 527–537.

67. Trifunac, M.D., Hao, T.Y. and Todorovska, M.I. (2001c). "On Energy Flow in Earthquake Response", Report CE 01-03, University of Southern California, Los Angeles, U.S.A.

68. Trifunac, M.D., Ivanović, S.S. and Todorovska, M.I. (2003). "Wave Propagation in a Seven-Story Reinforced Concrete Building. III. Damage Detection via Changes in Wavenumbers", Soil Dynamics and Earthquake Engineering, Vol. 23, No. 1, pp. 65–75.

69. Uang, C.M. and Bertero, V.V. (1988). "Use of Energy as a Design Criterion in Earthquake-Resistant Design", Report UCB/EERC-88/18, University of California, Berkeley, U.S.A.

70. Veletsos, A.S. and Newmark, N.M. (1960). "Effect of Inelastic Behavior on the Response of Simple Systems to Earthquake Motions", Proceedings of the Second World Conference on Earthquake Engineering, Tokyo, Japan, Vol. II, pp. 859–912.